ACS APPLIED MATERIALS & INTERFACES

Article

TiO2-BiVO4 heterostructure to enhance photoelectrochemical efficiency for sensitive aptasensing

Pei Pei Liu, Xiaoqiang Liu, Xiao He Huo, Yunfei Tang, Jun Xu, and Huangxian Ju

ACS Appl. Mater. Interfaces, **Just Accepted Manuscript** • DOI: 10.1021/acsami.7b07047 • Publication Date (Web): 31 Jul 2017

TiO_2-$BiVO_4$ heterostructure to enhance photoelectrochemical efficiency for sensitive aptasensing

Pei Pei Liu[a], Xiaoqiang Liu[a*], Xiao He Huo[a], Yunfei Tang[a], Jun Xu[a] and Huangxian Ju[b*]

[a] *Institute of Environmental and Analytical Sciences, College of Chemistry and Chemical Engineering, Henan University, Kaifeng, Henan Province, 475004, P.R. China*

[b] *State Key Laboratory of Analytical Chemistry for Life Science, Department of Chemistry, Nanjing University, Nanjing 210023, P.R. China*

Keywords: TiO_2-$BiVO_4$ heterostructure; Photoelectrochemical aptasensor; Sensitization; DNA aptamers; Nanobiosensing; 17β-estradiol

* Corresponding author. Phone/Fax: +86-25-89683593. E-mail address: xq_liu1975@yahoo.com (X. Liu); hxju@nju.edu.cn (H. Ju)

ABSTRACT: This work designed a nanocomposite to enhance the photoelectrochemical (PEC) efficiency by depositing $BiVO_4$ nanoparticles on TiO_2 nanospheres with a solvothermal method. The TiO_2-$BiVO_4$ heterostructure was characterized with various spectroscopic and microscopic techniques, and employed as a nanostructured support to cross-link DNA aptamer for constructing a visible-light driven PEC aptasensor. The TiO_2 nanospheres provided a biocompatible microenvironment, and the high surface area of heterostructure enhanced the loading of aptamer molecules. The small energy gap of $BiVO_4$ improved the PEC property of the nanocomposite compared with the pure TiO_2 under visible-light irradiation. The advantages of the nanocomposite along with the high loading of recognition molecules greatly improved the sensitivity of the aptasensor. Using 17β-estradiol as an analyst model, the proposed PEC biosensor showed excellent analytical performance with high sensitivity, low detection limit of 0.022 pM and high selectivity in a detectable concentration of range 0.1-250 pM, indicating the promising application of the designed TiO_2-$BiVO_4$ heterostructure in PEC biosensing.

■ INTRODUCTION

Steroid hormones have attracted great attention in environmental and biomedical fields due to their harmful effects on endocrine function of human and animals.[1] For example, the presence of low concentration of estrogens in the environment can cause abnormal sexual development of animals and decrease the average numbers of human spermatozoa.[2-3] Therefore, highly sensitive and selective detection of estrogens in aquatic environments is of great importance to protect the health of human and animals. The classical method for determination of estrogens is high-performance liquid chromatography,[1] but this technology requires rather complicated instrumentations, intensive labour and large amount of time. With the achievements of nanotechnology and nanoscience, nanobiosensing opens up the novel avenue for sensitive biosensing of in clinical, environmental, and industrial applications. Some electrochemical biosensors based on nanotechnology have been developed for sensitive detection of estrogen.[1] However, specific biosensors with high sensitivity for estrogen detection is still in urgent demand.

As a fast growing analytical technique, photoelectrochemical (PEC) detection has been paid great attention owing to its desirable signal to noise ratio, low cost and fast detection speed.[4-5] However, the poor sensitivity and selectivity of PEC sensors has restricted their further practical applications. To improve the sensitivity, various semiconductors, especially TiO_2-based composites have been applied in the construction of photocatalysis photovoltaic devices and biosensors owing to their high photon-to-electron conversion efficiency, excellent biocompatibility and remarkable chemical stability.[6] However, TiO_2 can only be excited by ultraviolet light (< 387nm), which occupies less than 5% of solar light spectrum. In addition, photo-induced hole-electron pairs in TiO_2 semiconductors are subjected to fast recombination.[7] The ideal way of minimizing these drawbacks is to combine other visible-light driven semiconductors with TiO_2. For example, Zhang et al.[2, 8] synthesized a graphene-TiO_2 nanocomposite as a visible light photocatalyst for selective oxidation of alcohols under mild conditions. The composite exhibited a much more active visible light photocatalytic activity than pure TiO_2. Inspired by this report, this work made use of the small band gap (~2.4 eV) of monoclinic $BiVO_4$ that has shown strong visible light excitation capability[9-10] to design a novel nanocomposite by depositing $BiVO_4$ nanoparticles on TiO_2 nanospheres with a solvothermal method. TiO_2 nanospheres were initially prepared by a sol-gel method. The relatively high conduction band (CB) edge position of $BiVO_4$ nanoparticles can facilitate the charge transfer when they are composited with other photo-materials with lower CB position.[11] The nanostructure of $BiVO_4$ avoids rapid recombination of photo-generated charges and poor charge transfer property of bulky $BiVO_4$.[12-13] The advantages of nanocomposite with strong visible light absorption led to high PEC efficiency for sensitive biosensing.

To obtaining specific response, this work further immobilized DNA aptamer on TiO_2-$BiVO_4$ heterostructure modified indium tin oxide (ITO) to recognize the target. Aptamers are artificial single-stranded DNA or RNA oligonucleotieds, which can selectively recognize various targets including small species, sugars, proteins and even whole cells,[14-15] and have shown superiority over the traditional recognition elements such as antibodies due to their unique features including simple preparation, easy preservation, good reproducibility, reversible denaturation, stability against high temperature and extreme pH, and particularly target versatility.[7, 16] It has been increasingly used as an attractive recognition element for the development of aptasensors.[2] Using 17β-estradiol (E2) as a model analyte, the fabricated PEC aptasensor showed excellent analytical performance over other PEC sensors. The high sensitivity and selectivity for detection of target indicated the promising application of the designed TiO_2-$BiVO_4$ heterostructure in PEC biosensing.

■ EXPERIMENTAL

Material and Reagents. All reagents were commercially available as analytical reagent grade and used as received unless otherwise stated. $Bi(NO_3)_3 \cdot 5H_2O$, NH_4VO_3 and ascorbic acid (AA) were purchased from Sinopharm chemical reagent Co., Ltd. (Shanghai, PR China). Titanium isopropoxide (TTIP, 97%+) and valeric acid were purchased from Alfa Aesar (China) Chemicals Co., Ltd. Chitosan (CS, 85% deacetylation) was ordered from Sigma-Aldrich Chemical Co. (St. Louis, MO). Ammonia (28%) , glutaraldehyde (50%), 1-aminoanthraquinone and bisphenol A were obtained from J&K Scientific Ltd. (Beijing, China). 17β-Estradiol (E2), estriol, ethinylestradiol, testosterone and bovine serum albumin (BSA) were purchased from Shanghai Sangon Biological Engineering Technological Co. Ltd. (Shanghai, China). The amino modified oligonucleotides were purchased from Shanghai Sangon Biotechnology Co. Ltd. (Shanghai, China) with the following sequence: 5´-GCT-TCC-AGC-TTA-TTG-AAT-TAC-ACG-CAG-AGG-GTA-GCG-GCT-CTG-C GC-ATT-CAA-TTG-CTG-CGC-GCT-GAA-GCG-CGG-AAG-C-3´. The aptamer was dissolved in phosphate buffer saline (PBS, pH 7.4) and kept frozen. In this work, 0.1 mol L^{-1} PBS (pH 7.4) was always employed as the supporting electrolyte for PEC determination. Ultrapure water obtained from a Millipore water purification system (≥18 MΩ cm^{-1}, Milli-Q, Millipore) was used throughout the whole experiments.

Apparatus. PEC measurements were performed in a conventional three-electrode system consisted of a modified ITO as working electrode, a platinum wire as auxiliary electrode, a saturated Ag|AgCl electrode (3.0 M KCl) as reference electrode. Potential was applied by a CHI630D Electrochemical Workstation (Shanghai CH Instruments, China) and a Xe lamp equipped with a 400 nm cut off filter (CEL-HXUV 300, Beijing AULTT, China) was used as the irradiation source. ITO electrodes were ordered from Wuhan Lattice Solar Energy Technology, Ltd., China. The morphology of the nanomaterials was examined by scanning electron microscopy (SEM, JSM-7500F, JEOL., Japan), transmision electron microscope (TEM, Tecnai G2 20, USA), X-ray powder diffraction (XRD, X-PertPro, Netherland) with a Cu Kα radiation (λ = 1.5406 nm). UV-vis diffuse reflectance spectra of the samples were measured on an UV-vis spectrophotometer (DRS, UV-2600, Kyoto, Japan). XPS were collected on an X-ray photoelectron spectrometer (ESCALAB 250Xi, USA) with a monochromated Al Kα source (hv =1486.6 eV), 150 W Power and 500 mm beam spot. The spectra were calibrated on the C1s peak (284.8 eV) and analysed with XPSPEAK41 software.

Preparation of TiO_2-$BiVO_4$ Composite. The synthesis of TiO_2-$BiVO_4$ composite was illustrated in Scheme 1A. In brief, 0.585 g of NH_4VO_3 and 2.425 g of $Bi(NO_3)_3$•$5H_2O$

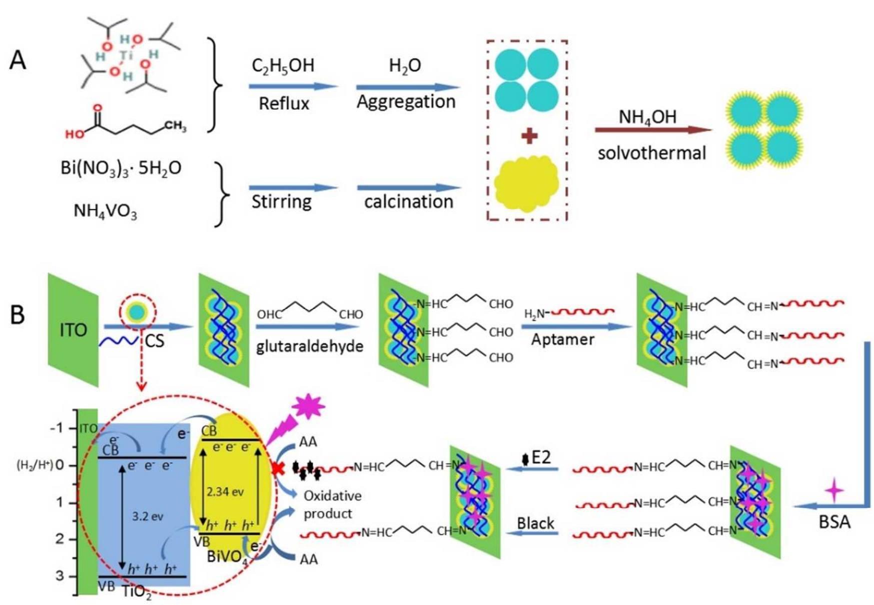

Scheme 1. (A) Synthesis of TiO_2-$BiVO_4$ composite, and (B) fabrication procedure of

aptasensor and photoelectrochemical mechanism in 0.1 M PBS containing 0.1 M AA.

were added into 100 mL water under stirring to produce a yellow precipitate, which was then filtered, washed with water, and dried overnight at 60 °C. Subsequently, the resulted product was placed into an alumina crucible and heated to 500 °C for 4 h to obtain the monoclinic $BiVO_4$. The precursor TiO_2 spheres were synthesized using a sol-gel method.[17] Firstly, 0.9 mL of valeric acid was added into 60 mL of ethanol, followed by the addition of 0.9 mL of TTIP to obtain a mixed solution, which was then stirred vigorously and heated at 80 °C for 6 h under reflux in the air. Next, hydrolysis and condensation were initiated by adding 6 mL water and 30 mL ethanol into the refluxed solution. After reaction for 4 hours, precursor TiO_2 spheres were precipitated, centrifuged, and then washed several times with ethanol and water. Finally, 0.2 g precursor TiO_2 spheres, 0.04 g $BiVO_4$ and 1.2 mL of NH_4OH (28% in water) were successively dispersed in a solution of 8 mL water and 30 mL ethanol. The dispersion was vigorously stirred for 1 h and then transferred to a 50 mL Teflon-lined stainless steel autoclave kept in an oven at 160 °C for 16 h. TiO_2-$BiVO_4$ composite was obtained after the dispersion was centrifuged, washed in ethanol and dried in an oven at 60 °C overnight.

Preparation of PEC Aptasensor. ITO electrode was cleaned with NaOH (1 M) and H_2O_2 (30%), then washed successively with acetone, alcohol and water under sonification before use. TiO_2-$BiVO_4$ composite (2 mg) was dispersed in 1 mL (0.1% w/v) chitosan aqueous solution containing 1% acetic acid for 1 h to obtain a suspension, 50 μL of which was then applied on ITO. After drying, TiO_2-$BiVO_4$|ITO was immersed into 2.5% (v/v) glutaraldehyde in water for 1 h， and thoroughly cleaned to remove the physically absorbed glutaraldehyde. Subsequently, 50 μL of aptamer (2 μM) was covalently immobilized onto the TiO_2-$BiVO_4$|ITO, which was then rinsed with PBS to remove the unbound aptamer and immersed into the BSA solution 3% (w/v) for 1 h to block nonspecific binding sites. The obtained aptasensor was stored at 4 ^{o}C overnight until use. The procedure for the biosensor fabrication is illustrated in Scheme 1B.

PEC Measurements. The PEC tests were performed in PBS (0.1 M, pH 7.4) solution containing 0.1 M KCl and 0.1 M AA at a bias voltage of 0.6 V with increasing concentration of E2. The current-time plots were recorded as the visible excitation light was switched on and off. Herein, AA served as an electron donor for capturing photo-generated holes to maintain the photocurrent stability of the PEC aptasensor.

■ RESULTS AND DISCUSSION

Characterization of Prepared Materials. The SEM and TEM images of $BiVO_4$, precursor TiO_2, and TiO_2-$BiVO_4$ composite were displayed to characterize their morphologies (Fig. 1). The $BiVO_4$ sample was composed of irregular particles with an average diameter of ~1 μm (Fig. 1a). The precursor TiO_2 sample consisted of uniform monodisperse beads with very smooth surface (Fig. 1b). From the magnified image of

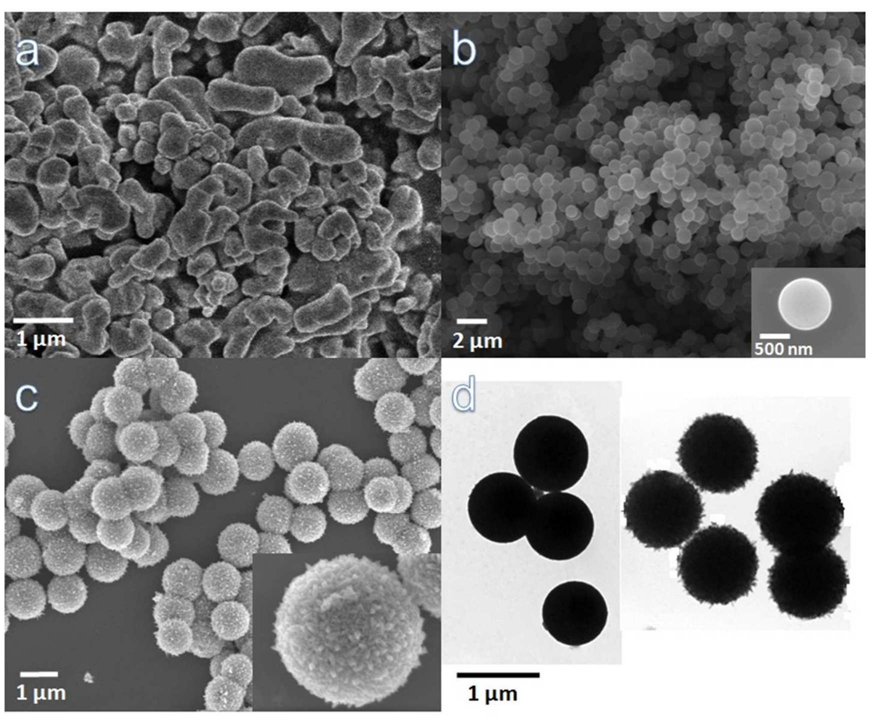

Fig. 1 SEM images of (a) $BiVO_4$, (b) precursor TiO_2, (c) TiO_2-$BiVO_4$ composite, and (d) TEM images of precursor TiO_2 (left) and TiO_2-$BiVO_4$ composite (right).

the precursor TiO_2 beads (inset of Fig. 1b), the average diameter of these TiO_2 microspheres was estimated to be 800 ± 50 nm. After the solvothermal treatment, the smooth precursor TiO_2 beads were transformed to the microspheres with rough surface and larger average diameter (1000 ± 50 nm), indicating the deposition of $BiVO_4$ nanoparticles on TiO_2 spheres (Fig. 1c). The TEM images (Fig. 1d) of precursor TiO_2 (left part) and TiO_2-$BiVO_4$ composite (right part) provided the similar results as the previous SEM images (Fig. 1b and 1c), which also confirmed the formation of the binary heterostructure. In addition, the SEM and TEM photos demonstrated the intimate contact between TiO_2 and $BiVO_4$, which facilitates the electron transfer within the binary composite and improve the separation of photo-generated charges.

The XRD pattern of precursor TiO_2 did not show any obvious diffraction peaks (Fig. 2A, curve a), indicating the amorphous structure of these TiO_2 spheres.[9] On the contrary, anatase TiO_2 exhibited several typical peaks at 25.3^o, 37.8^o, 48.0 ^{o}, 53.9 ^{o}, 55.1^o and 62.7^o (Fig. 2A, curve b), corresponding to the (101), (004), (200), (105), (211) and (204) crystal planes (JCPDS card 21-1272).[10] The XRD pattern of $BiVO_4$ showed the peaks at 18.9^o,

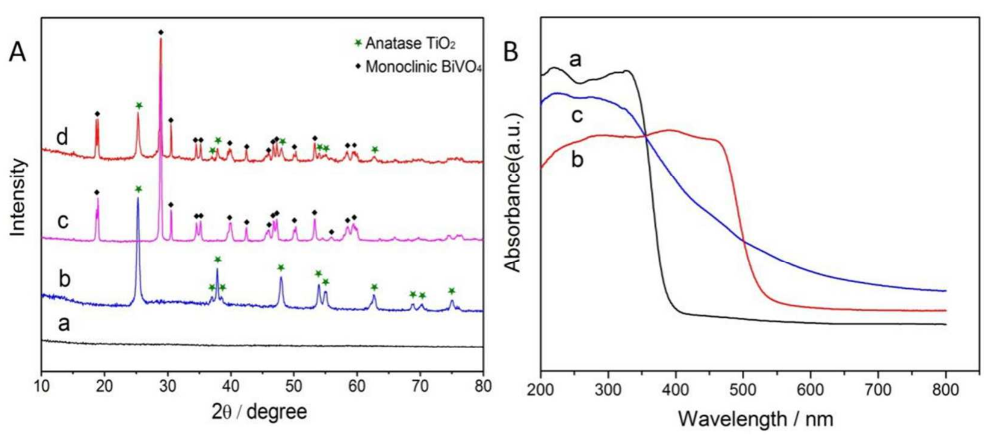

Fig. 2 (A) XRD patterns of (a) precursor TiO_2, (b) anatase TiO_2, (c) $BiVO_4$ and (d) TiO_2-$BiVO_4$

composite; (B) UV-vis diffuses reflectance spectra of (a) anatase TiO_2, (b) $BiVO_4$ and (c) TiO_2-$BiVO_4$ composite.

28.8°, 30.5°, 34.5°, 39.8° ,46.6°, 47.3° , 53.2 ° and 55.9° (Fig. 2A, curve c), which could be indexed to the characteristic (011) (112), (004), (200), (211), (204), (024), (116) and (215) crystal planes of monoclinic $BiVO_4$ (JCPDS No.14-0688), respectively.[18] Importantly, XRD pattern of TiO_2-$BiVO_4$ composite showed almost all the typical peaks ascribing to both anatase TiO_2 and monoclinic $BiVO_4$ (Fig. 2A, curve d), demonstrating the TiO_2 crystal transformation from amorphous to anatase and the successful deposition of monoclinic $BiVO_4$ on TiO_2 nanospheres. However, the peak intensity of $BiVO_4$ in curve d was obviously smaller than that in curve c, most likely due to the low percentage composition of $BiVO_4$ in the composite.

The DRS spectrum of anatase TiO_2 showed the absorption edge at 387 nm (Fig. 2B, curve a). According to the Scherer equation, $\lambda = 1240/E_g$ (λ was the absorption edge wavelength),[19] the band gap energy (E_g) was estimated to be 3.2 eV. From the UV-vis absorption edge of the prepared $BiVO_4$ at 530 nm (Fig. 2B, curve b), $BiVO_4$ was a visible light absorber with an E_g of 2.34 eV. Compared to the spectrum of anatase TiO_2, the absorption edge of TiO_2-$BiVO_4$ composite (Fig. 2B, curve c) was extended into the visible light region up to ~650 nm, which demonstrated the visible light adsorption capability of the composite.

The XPS measurements were also conducted to investigate the elemental composition of the composite. The XPS survey spectrum of TiO_2-$BiVO_4$ (Fig. 3a) showed the Ti 2p, Bi 4f, O 1s, and V 2p peaks, attributing to the typical elements of the composite. The peak at the binding energy of 980 eV was attributed to O KLL Auger peak at this energy.[20] The high-resolution spectrum of Ti 2p exhibited two peaks at 464.4 and 458.6 eV (Fig. 3b), which could be assigned to Ti $2p_{1/2}$ and Ti $2p_{3/2}$ of Ti^{4+} in anatase titania.[11] In Fig. 3c, two bands at 164.4 and 159.1 eV could be ascribed to the Bi $4f_{5/2}$ and Bi $4f_{7/2}$ binding energies respectively, which confirmed that the bismuth species in the composite belonged to Bi^{3+} cations.[12] The asymmetric O 1s signal (Fig. 3d) indicated the presence of different oxygen species on the surface of the sample, and the bands at 529.8 and 531.4 eV could be attributed to the surface lattice oxygen of TiO_2 and $BiVO_4$,[13] respectively. In Fig. 3e, the vanadium peaks centred at the binding energies of 516.6 (V $2p_{3/2}$) and 523.9 (V $2p_{1/2}$) eV demonstrated the existence of the characteristic V^{5+} oxidation state in the composite.[21] In summary, the XPS spectra validated the formation of $BiVO_4$ crystal on TiO_2.

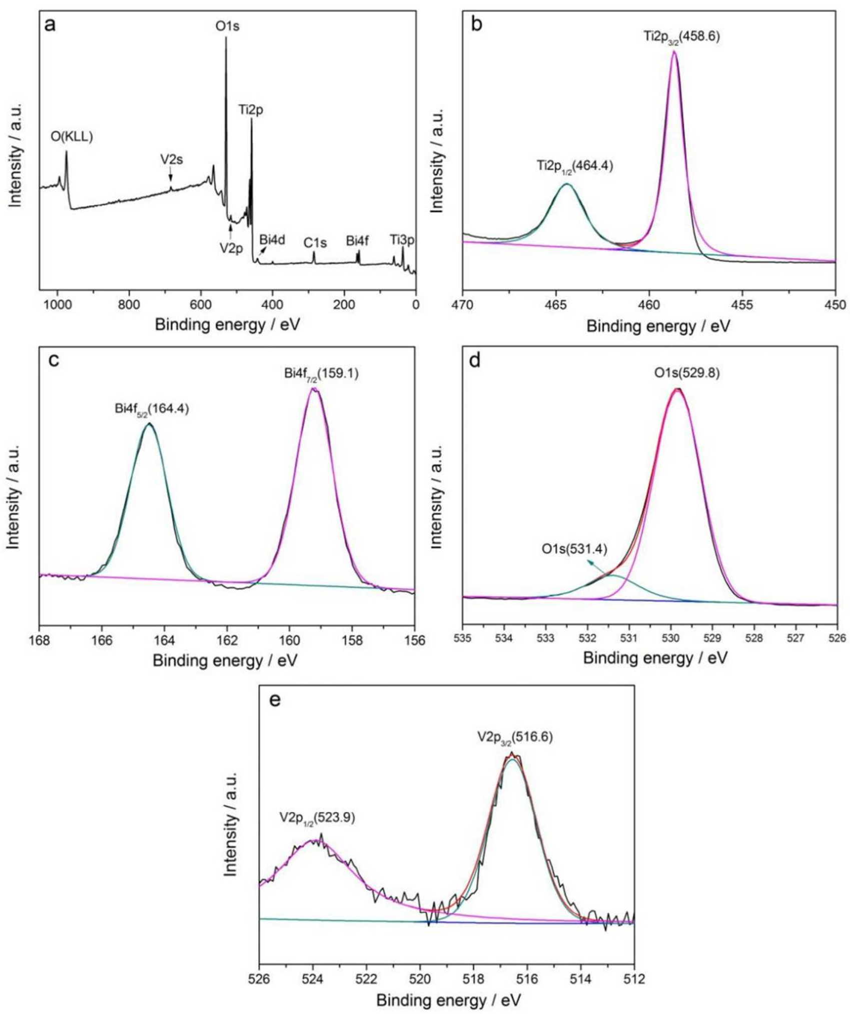

Fig. 3 (a) XPS survey scan of TiO_2-$BiVO_4$ composite, and high-resolution XPS spectra of (b) Ti2p,

(c) Bi4f, (d) O1s and (e) V2p.

Optimization of Aptasensor Preparation and Detection Potential. The response of the fabricated aptamer|TiO_2-$BiVO_4$|ITO sensor to E2 was optimized in 0.1 M PBS. Fig. 4A illustrates that the PEC response of the aptasensor is obviously affected by the concentration of aptamer immobilized on the electrode. Specifically, the PEC response difference ($\Delta I = I - I_0$, I_0 is the blank photocurrent) toward E2 markedly increased with the increase of aptamer concentration up to 2 μM probably because higher concentration of aptamer immobilized on the electrode could capture more E2 molecules. However, the ΔI reached a platform when the aptamer concentration exceeds 2 μM, which could be ascribed to the steric hindrance of excessive aptamer retarding the electron transfer.[22] Consequently, aptamer at 2 μM was chosen to fabricate the sensor. Meanwhile, the bias potential also showed an obvious effect on the PEC response of the sensor (Fig. 4B). The response rapidly increased with enhancing the bias potential from +0.2 to +0.6 V because larger anodic bias potential will push more photo-generated electrons to the counter electrode and reduce the recombination of hole-electron pairs more effectively, leading to higher photocurrent. However, the enhancement of PEC response was significantly slowed down at applied potential higher than + 0.6 V and therefore + 0.6 V was selected as the optimum applied potential for PEC sensing to minimize the interference arising from the high potentials.

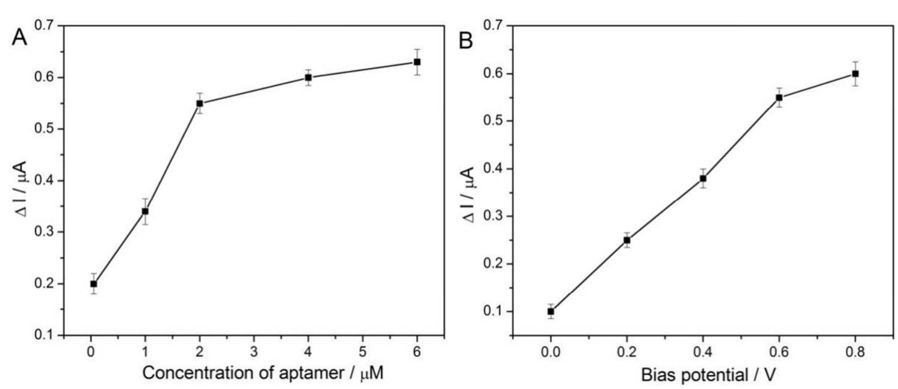

Fig. 4 Influence of (A) aptamer concentration and (B) bias potential on PEC response of aptamer|TiO_2-$BiVO_4$|ITO to 60 pM E2 in 0.1 M PBS containing 0.1 M AA.

Analytical Performance of PEC Aptasensor. The PEC performance of different modified ITO electrodes was evaluated by studying the photocurrents generated by irradiating the electrodes with intermittent visible incident light (Fig. 5A). The photocurrent at TiO_2-$BiVO_4$|ITO (curve c) was ~1.8 times larger than that at TiO_2|ITO (curve a), attributing to that $BiVO_4$ particles has extended the absorption of TiO_2 spheres into the visible light region. In the composite, the conduction band edge potential of $BiVO_4$ (~ -0.7 eV) was more negative than that of TiO_2 (~ -0.4 eV),[23] so that the photo-

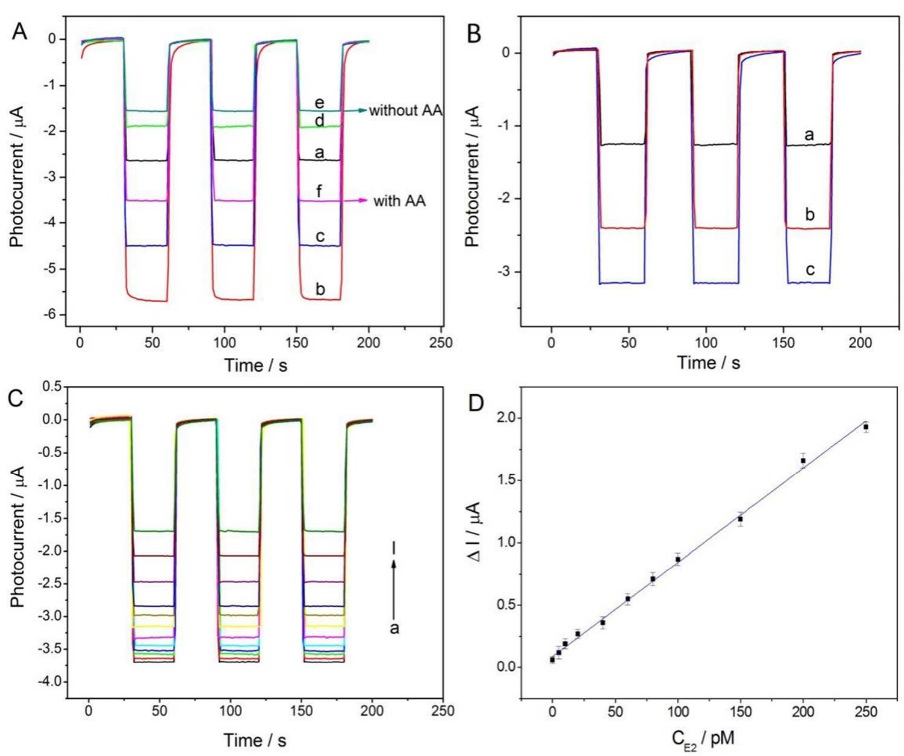

Fig. 5 (A) Photocurrents at (a) TiO_2|ITO, (b) $BiVO_4$|ITO, (c) TiO_2-$BiVO_4$|ITO, (d) aptamer|TiO_2-$BiVO_4$|ITO in 0.1 M PBS (pH 7.4), and aptamer|TiO_2-$BiVO_4$|ITO in 0.1 PBS (pH 7.4) containing 10 pM E2 before (e) and after (f) addition of 0.1 M AA. (B) Photocurrents at (a) aptamer|TiO_2|ITO, (b) aptamer|$BiVO_4$|ITO and (c) aptamer|TiO_2-$BiVO_4$|ITO in 0.1 M PBS (pH 7.4)

containing 60 pM E2 and 0.1 M AA. (C) Photocurrent at PEC aptasensor in PBS (0.1 M, pH 7.4) containing 0, 0.1, 5, 10, 20, 40, 60, 80, 100, 150, 200 and 250 pM E2 (from a to l) in the presence of 0.1 M AA at a bias voltage of + 0.6 V; (D) Plot of ΔI and E2 concentration from 0.1 to 250 pM.

induced electrons on the conduction band of $BiVO_4$ was easily transferred to that of TiO_2 to improve the PEC conversion efficiency of TiO_2.[24] However, the photocurrent at TiO_2-$BiVO_4$|ITO (curve c) is lower than that at $BiVO_4$|ITO (curve b), which can be explained by the substantial charge carrier loss of $BiVO_4$ on the TiO2 nanospheres.[25] Noticeably, aptamer|TiO_2-$BiVO_4$|ITO (curve d) displays the lowest photocurrent among all the modified electrodes owing to the steric hindrance of the biological molecules on ITO. The steric hindrance of biological retarded the movement of photogenerated electrons to ITO and thus increased their recombination with the holes. After 0.1 M AA was added in PBS (pH 7.4) containing 10 pM E2, the photocurrent at aptamer|TiO_2-$BiVO_4$|ITO was almost doubled (curve e and f), which was ascribed the fact that AA served as a scavenger of photo-generated holes to enhance and stabilize the photocurrent at the PEC aptasensor. To reduce the irradiation absorbance of AA at high concentration, 0.1 M AA was chosen for the subsequent test.

Compared to aptamer|TiO_2|ITO and aptamer|$BiVO_4$|ITO, aptamer|TiO_2-$BiVO_4$|ITO showed the highest photocurrent in PBS containing 60 PM of E2 (Fig. 5B), indicating that the TiO_2-$BiVO_4$ heterostructure significantly enhanced the PEC efficiency for aptasensing. The result could be attributed to the strong visible-light excited capability, high specific surface area and excellent biocompatibility of TiO_2-$BiVO_4$ heterostructure.

To evaluate the performance of the E2 PEC aptasensor, the photocurrent change was measured at various concentrations of E2. As shown in Fig. 5C, the photocurrent gradually decreased with increasing concentrations of E2. Ascribing to the specific recognition reaction between E2 and aptamer, the E2-aptamer complexes were formed on the PEC sensing interface, which increased the steric hindrances for the diffusion of the electron donor and thus decreased the photocurrent. The plot of ΔI vs E2 concentration showed a linear relationship (Fig. 5D). The photocurrent changed linearly with the concentration of E2 in the range from 0.1 to 250 pM (correlation coefficient of 0.998) with a detection limit of 0.022 pM (S/N=3). The performance of as prepared PEC sensor was superior to those of many other sensors (Table 1), which could be attributed to the excellent property of TiO_2-$BiVO_4$ composite.

Table 1 Analytical performance of different sensors for the detection of E2.

Sensors	Analytical technique	Linear range / pM	LOD / pM	References
[1]TiP@Cd^{2+}/ITO	PEC	18 - 1.4×10^4	7.3	2
Aptamer/AuNPs[2]/WS_2[3]/GCE[4]	DPV	10 - 5.0×10^3	2.0	3
Aptamer/CdSe-TiO_2	PEC	0.05 - 15	3.3×10^{-2}	4
Aptamer/α-Fe_2O_3-NG[5]-AuNRs/ ITO	PEC	1.0×10^{-3} - 1.0×10^3	3.3×10^{-4}	5
Ag/PAMAM[6]-Au/GR[7]-PANI[8]/ GCE	DPV	1.4×10^2 – 2.5×10^4	72	7
CdSe–BSA–E2/GCE	DPASV	1.8×10^2 - 3.67×10^3	1.8×10^2	8
cDNA/Aptamer/AuNPs/ CoS/GCE	DPV	1 - 1000	0.7	9
Aptamer/AuNPs/PEDOT[9]/Au	SWV	100 - 1×10^5	20	10
Aptamer/Au	EIS	10 - 1×10^4	2.0	11
Aptamer|TiO_2-$BiVO_4$| ITO	PEC	0. 1 - 250	2.5×10^{-2}	this work

[1] Cd^{2+}-functionalized titanium phosphate nanoparticles; [2] Au nanoparticles; [3] layered tungsten disulfide; [4] glassy carbon electrode; [5] N-doped graphene; [6] poly(amino-amine) dendrimers; [7] graphene; [8]polyaniline; [9] Poly(3,4-ethylenedioxylthiophene).

The PEC mechanism of the biosensing strategy was illustrated in Scheme 1(B) based on inter-particle electron transfer behavior. The band edge positions of the conduction band (CB) and valence band (VB) of a semiconductor could be estimated according to the equation $E_{CB} = \chi - E^0 - 1/2E_g$, where χ is the absolute electronegativity of the compound, and E^0 is the energy of free electron on the hydrogen scale and E_g is the band gap of the semiconductor.[23] From Fig. 2B, the band gaps of TiO_2 and $BiVO_4$ were calculated to be 3.2 eV and 2.34 eV, respectively. Therefore, the CB and VB edges of TiO_2 were calculated to be -0.2 eV and 3.0 eV, and those of $BiVO_4$ were 0.37 and 2.71 eV, respectively. After $BiVO_4$ and TiO_2 were joined to form a heterostructure, the Fermi levels of two components tended to a balanced value due to the charge redistribution and system thermal equilibrium.[26,27] Consequently, both the CB and VB of $BiVO_4$ moved to the positions negative to those of TiO_2,[28,29] facilitating the migration of the photo-generated electrons of $BiVO_4$ to the CB of TiO_2 and then to the ITO electrodes. Meanwhile, the photo-induced holes on the VB of TiO_2 could also be injected into that of $BiVO_4$ and then captured by an electron donor AA. The effective separation between the electrons and holes in the composite maintained the photocurrent stability of the PEC aptasensor, leading to a much better PEC performance of the TiO_2-$BiVO_4$ composite than that of pristine TiO_2 nano-materials.

Stability, specificity and practical application. The stability of the PEC aptasensor was evaluated through monitoring the repeated photoexcited process 7 times over 420 s. In 0.1 mol L^{-1} PBS (pH 7.4), the photocurrent did not show any obvious change at a bias voltage of 0.6 V under the irradiation, indicating the high stability of the PEC sensor (Fig. 6A). The selectivity evaluation of the PEC aptasensor for 17β-estradiol was performed

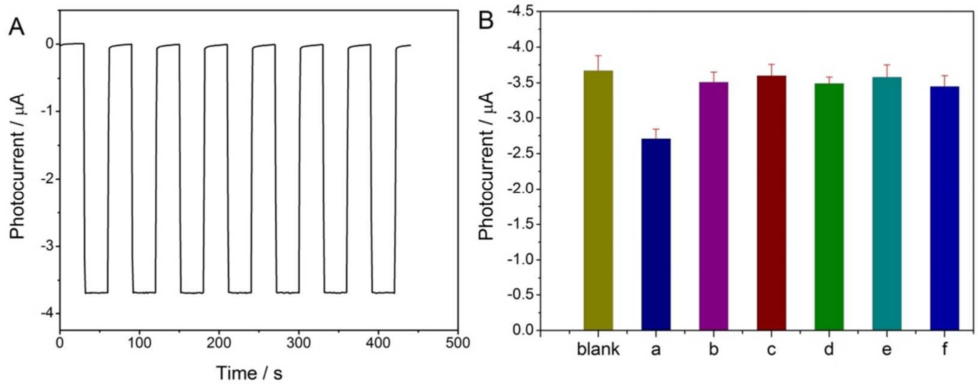

Fig. 6 (A) Time based photocurrent response of aptamer|TiO_2-$BiVO_4$|ITO under several on/off irradiation cycles for 420 s; (B) The photocurrent of the prepared PEC E2 aptasensor to (a) 10 pM E2, and 50 pM of (b) estriol, (c) 1-aminoanthraquinone, (d) ethinylestradiol, (e) testosterone and (f) bisphenol A.

by testing the response of the sensor to some other common co-existed species including estriol, 1-aminoanthraquinone, ethinylestradiol, testosterone and bisphenol A. The influences of these potential interferences on the determination of E2 were less than 6.7%, (Fig. 6B), indicating the high selectivity of the PEC aptasensor for E2.

The long-term storage stability of the aptamersensor was investigated after storing the aptamersensor in a refrigerator at 4 □. The aptamersensor retained 92.5% and 86.5% of the initial response after two weeks and four weeks' refrigerator storage respectively. The good stability of the sensor was attributed to tight immobilzation of aptamer on the biocompatible sensor scaffold, which could retain the biological activity of biological molecules.

The practical application of the developed biosensor was studied by detecting 17β-estradiol in human urine samples collected from three volunteers. The human urine samples were diluted 100 times with PBS and the standard addition method was used to quantitative analyse these samples. As listed in Table 2, the recoveries of the proposed method for these urine samples are in the range from 96.4 to 103.2%, demonstrating that the proposed sensor could be applied in practical determination of 17β-estradiol.

Table 2 Determination of 17β-estradiol in urine samples (*n* = 3).

Samples	Spiked (pM)	Found (pM)	RSD (%)	Recovery (%)
1	5	4.82	1.6	96.4
	15	15.22	2.4	100.3
	30	30.17	1.9	99.4
2	5	5.27	3.2	101.2
	15	15.28	2.6	100.5
	30	30.31	2.8	100.3
3	5	5.07	3.5	98.4
	15	15.05	2.4	99.3
	30	30.96	3.0	103.2

■ CONCLUSION

We have prepared a TiO_2-$BiVO_4$ sphere heterostructure to develop a PEC aptamersensor, which displays high sensitivity, selectivity and stability for simple and rapid determination of 17 β-estradiol. In the designed heterostructure, TiO_2 nanospheres provide biocompatible microenvironment to maintain the aptamer bioactivity, and the high surface area of heterostructure enhances the loading of aptamer molecules. The advantages of the nanocomposite with strong visible light absorption lead to high PEC efficiency for sensitive biosensing. The fabricated PEC aptasensor possesses excellent analytical performance, and indicates that TiO_2-$BiVO_4$ heterostructure is a promising candidate for preparation of PEC biosensors.

■ ACKNOWLEDGMENTS

This work was financially supported by National Natural Science Foundation of China (No. U1504215，21576071), International Science and Technology Cooperative Project funded by

The Department of Science and Technology of Henan Province (172102410042) and the Scientific Research Foundation for the Returned Overseas Chinese Scholars, State Education Ministry Batch 46th.

■ AUTHOR INFORMATION

Corresponding Authors

*Phone/Fax: +86-25-89683593, e-mail: xq_liu1975@yahoo.com；hxju@nju.edu.cn

Notes

The authors declare no competing financial interest.

■ REFERENCES

(1) Fan, L.; Zhao, G.; Shi, H.; Liu, M.; Wang, Y.; Ke, H. A Femtomolar Level and Highly Selective 17β-Estradiol Photoelectrochemical Aptasensor Applied in Environmental Water Samples Analysis. *Environ. Sci. Technol.* **2014,** *48*, 5754-5761.

(2) Li, R.; Liu, Y.; Yan, T.; Li, Y.; Cao, W.; Wei, Q.; Du, B. A Competitive Photoelectrochemical Assay for Estradiol Based on in Situ Generated Cds-Enhanced TiO_2. *Biosens. Bioelectron.* **2015,** *66*, 596-602.

(3) Chang, H.-S.; Choo, K.-H.; Lee, B.; Choi, S.-J. The Methods of Identification, Analysis, and Removal of Endocrine Disrupting Compounds (EDCs) in Water. *J. Hazard. Mater.* **2009,** *172*, 1-12.

(4) Wang, G.-L.; Jiao, H.-J.; Liu, K.-L.; Wu, X.-M.; Dong, Y.-M.; Li, Z.-J.; Zhang, C. A Novel Strategy for the Construction of Photoelectrochemical Sensors Based on Quantum Dots and Electron Acceptor: The Case of Dopamine Detection. *Electrochem. Commun.* **2014,** *41*, 47-50.

(5) Hu, Y.; Xue, Z.; He, H.; Ai, R.; Liu, X.; Lu, X. Photoelectrochemical Sensing for Hydroquinone Based on Porphyrin-Functionalized Au Nanoparticles on Graphene. *Biosens. Bioelectron.* **2013,** *47*, 45-49.

(6) Giordano, F.; Abate, A.; Correa Baena, J. P.; Saliba, M.; Matsui, T.; Im, S. H.; Zakeeruddin, S. M.; Nazeeruddin, M. K.; Hagfeldt, A.; Graetzel, M. Enhanced Electronic Properties in Mesoporous TiO_2 Via Lithium Doping for High-Efficiency Perovskite Solar Cells. *Nat. Commun.* **2016,** *7*, 10379-.

(7) Yildirim, N.; Long, F.; Gao, C.; He, M.; Shi, H.-C.; Gu, A. Z. Aptamer-Based Optical Biosensor for Rapid and Sensitive Detection of 17β-Estradiol in Water Samples. *Environ. Sci. Technol.* **2012,** *46*, 3288-3294.

(8) Li, H.; Wang, D.; Fan, H.; Jiang, T.; Li, X.; Xie, T. Synthesis of Ordered

Multivalent Mn-TiO_2 Nanospheres with Tunable Size: A High Performance Visible-Light Photocatalyst. *Nano Res.* **2011,** *4*, 460-469.

(9) Abdi, F. F.; Han, L.; Smets, A. H. M.; Zeman, M.; Dam, B.; van de Krol, R. Efficient Solar Water Splitting by Enhanced Charge Separation in a Bismuth Vanadate-Silicon Tandem Photoelectrode. *Nat. Commun.* **2013,** *4*, 2195.

(10) Ding, C.; Qin, W.; Wang, N.; Liu, G.; Wang, Z.; Yan, P.; Shi, J.; Li, C. Solar-to-Hydrogen Efficiency Exceeding 2.5% Achieved for Overall Water Splitting with an All Earth-Abundant Dual-Photoelectrode. *Phys. Chem. Chem. Phys.* **2014,** *16*, 15608-15614.

(11) Sun, S.; Wang, W.; Zhou, L.; Xu, H. Efficient Methylene Blue Removal over Hydrothermally Synthesized Starlike $BiVO_4$. *Ind. Eng. Chem. Res.* **2009,** *48*, 1735-1739.

(12) Yehezkeli, O.; Harguindey, A.; Domaille, D. W.; He, L.; Cha, J. N. Synthesis and Phase Transfer of Well-Defined $BiVO_4$ Nanocrystals for Photocatalytic Water Splitting. *RSC Adv.* **2015,** *5*, 58755-58759.

(13) Shu, J.; Qiu, Z.; Lin, Z.; Cai, G.; Yang, H.; Tang, D. Semiautomated Support Photoelectrochemical Immunosensing Platform for Portable and High-Throughput Immunoassay Based on Au Nanocrystal Decorated Specific Crystal Facets $BiVO_4$ Photoanode. *Anal. Chem.* **2016,** *88*, 12539-12546.

(14) Huang, K.-J.; Liu, Y.-J.; Zhang, J.-Z.; Cao, J.-T.; Liu, Y.-M. Aptamer/Au Nanoparticles/Cobalt Sulfide Nanosheets Biosensor for 17β-Estradiol Detection Using a Guanine-Rich Complementary DNA Sequence for Signal Amplification. *Biosens. Bioelectron.* **2015,** *67*, 184-191.

(15) Li, H.; Qiao, Y.; Li, J.; Fang, H.; Fan, D.; Wang, W. A Sensitive and Label-Free Photoelectrochemical Aptasensor Using Co-Doped ZnO Diluted Magnetic

Semiconductor Nanoparticles. *Biosens. Bioelectron.* **2016,** *77*, 378-384.

(16) Ahour, F.; Ahsani, M. K. An Electrochemical Label-Free and Sensitive Thrombin Aptasensor Based on Graphene Oxide Modified Pencil Graphite Electrode. *Biosens. Bioelectron.* **2016,** *86*, 764-769.

(17) Tsai, M.-C.; Tsai, T.-L.; Shieh, D.-B.; Chiu, H.-T.; Lee, C.-Y. Detecting HER2 on Cancer Cells by TiO_2 Spheres Mie Scattering. *Anal. Chem.* **2009,** *81*, 7590-7596.

(18) Jung, H.; Chae, S. Y.; Shin, C.; Min, B. K.; Joo, O.-S.; Hwang, Y. J. Effect of the $Si/TiO_2/BiVO_4$ Heterojunction on the Onset Potential of Photocurrents for Solar Water Oxidation. *ACS Appl. Mater. Interfaces* **2015,** *7*, 5788-5796.

(19) Li, X.; Zhang, Z.; Zhang, F.-J.; Liu, J.; Ye, J.; Oh, W.-C. Synthesis and Photocatalytic Activity of $TiO_2/BiVO_4$ Layered Films under Visible Light Irradiation. *J. Korean Ceram. Soc* **2016,** *53*, 665-669.

(20) Zong, M.; Huang, Y.; Wu, H.; Zhao, Y.; Wang, Q.; Sun, X. One-Pot Hydrothermal Synthesis of $RGO/CoFe_2O_4$ Composite and Its Excellent Microwave Absorption Properties. *Mater. Lett.* **2014,** *114*, 52-55.

(21) Chen, D.; Huang, F.; Cheng, Y.-B.; Caruso, R. A. Mesoporous Anatase TiO_2 Beads with High Surface Areas and Controllable Pore Sizes: A Superior Candidate for High-Performance Dye-Sensitized Solar Cells. *Adv. Mater. (Weinheim, Ger.)* **2009,** *21*, 2206-2210.

(22) Liu, Y.; Yan, K.; Okoth, O. K.; Zhang, J. A Label-Free Photoelectrochemical Aptasensor Based on Nitrogen-Doped Graphene Quantum Dots for Chloramphenicol Determination. *Biosens. Bioelectron.* **2015,** *74*, 1016-1021.

(23) Sun, J.; Li, X.; Zhao, Q.; Tade, M. O.; Liu, S. Quantum-Sized $BiVO_4$ Modified TiO_2 Microflower Composite Heterostructures: Efficient Production of Hydroxyl Radicals Towards Visible Light-Driven Degradation of Gaseous Toluene. *J. Mater.*

Chem. A **2015,** *3*, 21655-21663.

(24) Zhang, L.; Tan, G.; Wei, S.; Ren, H.; Xia, A.; Luo, Y. Microwave Hydrothermal Synthesis and Photocatalytic Properties of TiO_2/$BiVO_4$ Composite Photocatalysts. *Ceram. Int.* **2013,** *39*, 8597-8604.

(25) Wang, R.; Bai, J.; Li, Y.; Zeng, Q.; Li, J.; Zhou, B. $BiVO_4$/TiO_2(N_2) Nanotubes Heterojunction Photoanode for Highly Efficient Photoelectrocatalytic Applications. *Nano-Micro Lett.* **2016,** *9*, 14-19.

(26) Hu, Y.; Li, D.; Zheng, Y.; Chen, W.; He, Y.; Shao, Y.; Fu, X.; Xiao, G. $BiVO_4$/TiO_2 Nanocrystalline Heterostructure: A Wide Spectrum Responsive Photocatalyst Towards the Highly Efficient Decomposition of Gaseous Benzene. *Appl. Catal., B* **2011,** *104*, 30-36.

(27) Sun, J.; Li, X.; Zhao, Q.; Ke, J.; Zhang, D. Novel V_2O_5/$BiVO_4$/TiO_2 Nanocomposites with High Visible-Light-Induced Photocatalytic Activity for the Degradation of Toluene. *J. Phys. Chem. C* **2014,** *118*, 10113-10121.

(28) Zhang, C.; Guo, D.; Xu, W.; Hu, C.; Chen, Y. Radiative/Nonradiative Recombination Affected by Defects and Electron–Phone Coupling in $CdWO_4$ Nanorods. *J. Phys. Chem. C* **2016,** *120*, 12218-12225.

(29) Zhang, C.; Zhang, H.; Zhang, K.; Li, X.; Leng, Q.; Hu, C. Photocatalytic Activity of Znwo4: Band Structure, Morphology and Surface Modification. *ACS Appl. Mater. Interfaces* **2014,** *6*, 14423-14432.

For Table of Contents Only